JOURNAL OF APPLIED ELECTROCHEMISTRY 24 (1994) 212–218

Mathematical modelling of electrode growth

J. DECONINCK

Department of Electrical Engineering, Vrije Universiteit Brussel, Pleinlaan 2, 1050 Brussels, Belgium

Received 22 January 1993; revised 25 July 1993

It is known that during electrodeposition or dissolution electrode shape change depends on the local current density (Faraday's law in differential form). Assuming that concentration gradients in the bulk of the solution may be neglected, the current distribution in an electrochemical system can be modelled by a Laplace equation (describing charge transport) with nonlinear boundary conditions caused by activation and concentration overpotentials on the electrodes. To solve this numerical problem, an Euler scheme is used for the integration of Faraday's law with respect to time and the field equation is discretized using the boundary element method (BEM). In this way, and by means of a specially developed electrode growth algorithm, it is possible to simulate electrodeposition or electrode dissolution. In particular, attention is paid to electrode variation in the vicinity of singularities. It is pointed out that the angle of incidence between an electrode and an adjacent insulator becomes right ($\pi/2$). This is confirmed by several experiments.

List of symbols

$\bar{x}_i$ coordinates of a point i belonging to a boundary (m)
t time (s)
$\bar{h}$ thickness variation at a point belonging to an electrode (m)
M molecular weight (kg mol^{-1})
ρ_m specific weight (kg m^{-3})
z charge of an ion (C)
F Faraday's constant (C mol^{-1})
R_{a2} impedance of the linearized activation overvoltage on cathode (Ω cm^{-2})
θ efficiency of the reaction
σ electric conductivity (Ω^{-1} m^{-1})
U electric potential (V)
$\bar{u}$ rate of mechanical displacement of a point (m s^{-1})
V applied potential on an electrode (V)
W Wagner number defined as the ratio of the mean impedance of the reaction $\frac{\partial \eta}{\partial J}|_{Jav}$ and the mean ohmic resistance of the cell given by L/σ with L a characteristic length of the cell.
η overvoltage (V)
η_1 overvoltage on anode (V)
η_2 overvoltage on cathode (V)

1. Introduction

Electrode shape changes due to electrodeposition and electrodissolution with simultaneous mechanical displacement of electrodes, as encountered in electrochemical machining, can be described by the following equation and boundary conditions [1, 2]

$$\frac{d\bar{h}(\bar{x}_i, t)}{dt} = -\theta \frac{M}{\rho_m z F} \sigma \frac{\partial U(\bar{x}_i, t)}{\partial n} \bar{l}_n + \bar{u}(\bar{x}_i, t) \qquad (1)$$

with $\bar{h}(\bar{x}_i, t = 0) = 0$. In this equation the following are applicable:
$\bar{h}(\bar{x}_i, t)$ is the thickness variation at each point $\bar{x}_i$ of the boundary (m);
$\theta(M/\rho_m z F)$ is the removal or growth rate (m^3 A^{-1} s^{-1});
σ is the electrolyte conductivity (Ω^{-1} m^{-1});
$\partial(U(\bar{x}_i, t)/\partial n)\bar{l}_n$ is the normal electric field at each point $\bar{x}_i$ of the boundary (V m^{-1});
$\bar{u}(\bar{x}_i, t)$ is the rate and the direction of the displacement of each point $\bar{x}_i$ of the boundary (m s^{-1}) with respect to a fixed reference point. Without loss of generality, $\bar{u}(\bar{x}_i, t) = 0$ in the following.

The boundary and the domain (the solution) change in time and, when concentration gradients in the solution can be omitted, at each moment the normal electric field satisfies the following equation and boundary conditions

$$\begin{aligned} &\bar{\nabla} \cdot (-\sigma \bar{\nabla} U) = 0 && \text{in the solution} \\ &\frac{\partial U}{\partial n}(\bar{x}_i, t) = 0 && \text{on insulating boundaries} \\ &\underline{U}(\bar{x}_i, t) = V - \eta_1 && \text{on the anode} \\ &\underline{U}(\bar{x}_i, t) = -\eta_2 && \text{on the cathode.} \end{aligned} \qquad (2)$$

In these equations, V is the applied voltage and η_1 and η_2 are the nonlinear overvoltages on the anode and cathode, respectively.

When the conductivity is constant, as is often encountered, it is well known [3–5] that for the solution of Equation 2, the boundary element method (BEM) is the most natural technique since only data on the boundaries are needed and used. The boundary element method requires only a discretization of the boundary into elements having nodal points (Fig. 1). To integrate Equation 1 a simple forward difference equation was used [6–9]. In this paper only aspects of electrode growth in the vicinity of singularities will be considered.

0021-891X

2. Simulation of electrode shape change next to an insulator

When the shape changes are small with respect to the element sizes and when no singularities are considered, the simulation is rather simple because there always exists a one to one relation between a nodal point at each time step. In the general case, several problems encountered at the electrode extremities require careful treatment. In the following only electrode growth is discussed. Depending on the angle of incidence at time step $n(\theta_n)$ between insulator and electrode there are two possibilities. Figures 1 and 2 represent part of an electrode near to an insulating boundary.

When the internal angle θ_n between electrode and insulator is smaller than or equal to $\pi/2$, (Fig. 1(a)), the new electrode profile at timestep t_{n+1} will intersect the boundary. In this case the coordinates of the intersection are to be calculated and elements and nodal points are changed (or cancelled) to obtain the configuration of Fig. 1(b).

On the other hand, as represented in Fig. 2(a), the internal angle θ_n between electrode and insulator can be larger than $\pi/2$. At the following timestep $n+1$, the new boundary is no longer closed. This is physically not correct and mathematically not allowed. In Fig. 2(b) and (c), two straightforward methods are shown to maintain the boundary closed. In Fig. 2(b) the new electrode profile at timestep t_{n+1} is obtained by introducing two elements between the new and the old extremity of the electrode. There is no overgrowth, in contrast with Fig. 2(c) where it is supposed that the electrode may be extrapolated to the boundary. Although the reality will be somewhere between these extremes, there are more arguments for accepting the idea

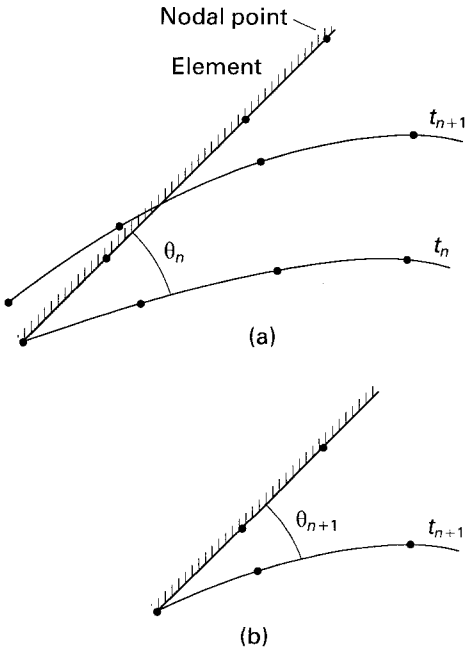

Fig. 1. Shape change near a contact between an electrode and an insulator when $\theta_n \leq \pi/2$; (a) before rearrangement of the discretized boundary, and (b) after rearrangements of elements.

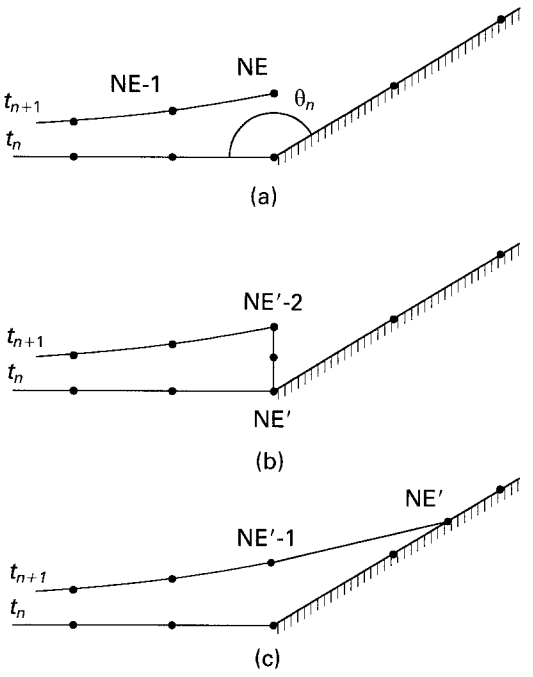

Fig. 2. Shape change near a contact between an electrode and an insulator when $\theta_n > \pi/2$; (a) before rearrangement of the discretized boundary, (b) connection is applied to keep the boundary closed, and (c) extrapolation is applied to keep the boundary closed.

of Fig. 2(b). A further possibility, which will be discussed later, was introduced by Ducovic [8].

Using the two mentioned possibilities to maintain the boundary closed, the deposition on the cathode was simulated in a Hull cell with the following dimensions: anode 6 cm, cathode 10 cm, shortest and longest distance between electrodes 5 cm and 13 cm. On the anode no overvoltage was considered because of its minor influence on the current density distribution on the cathode. On the cathode a small and a large linearized overvoltage were applied ($\eta_2 = R_{a2} J$ with J the local current density). At this stage linearization is justified as only general concepts are explained. The electrical conductivity σ of the solution was $0.25\,\Omega^{-1}\,\mathrm{cm}^{-1}$ and 1 V was applied between both electrodes. The results of these simulations, calculated with the data given in Table 1, are shown in Fig. 3(a)–(d).

Figure 3(a) and (c) were obtained by keeping the boundary closed by extrapolation, according to Fig. 2(c). In Fig. 3(a) the current density distribution is influenced by both the geometry of the cell and the overvoltage η_2. A non-negligible overpotential was introduced, only in order to see the evolution of the simulated electrode profile. Without an overpotential on the cathode the phenomenon seen here

Table 1. Numerical data applied for the simulations of Fig. 3(a)–(d)

Numerical data	$R_{a2}/(\Omega\,\mathrm{cm}^{-2})$	L/cm	$W = R_{a2}\sigma/L$
Fig. 3(a)	10	5	0.5
Fig. 3(b)	0.01	5	0.005
Fig. 3(c)	10000	5	500
Fig. 3(d)	10000	5	500

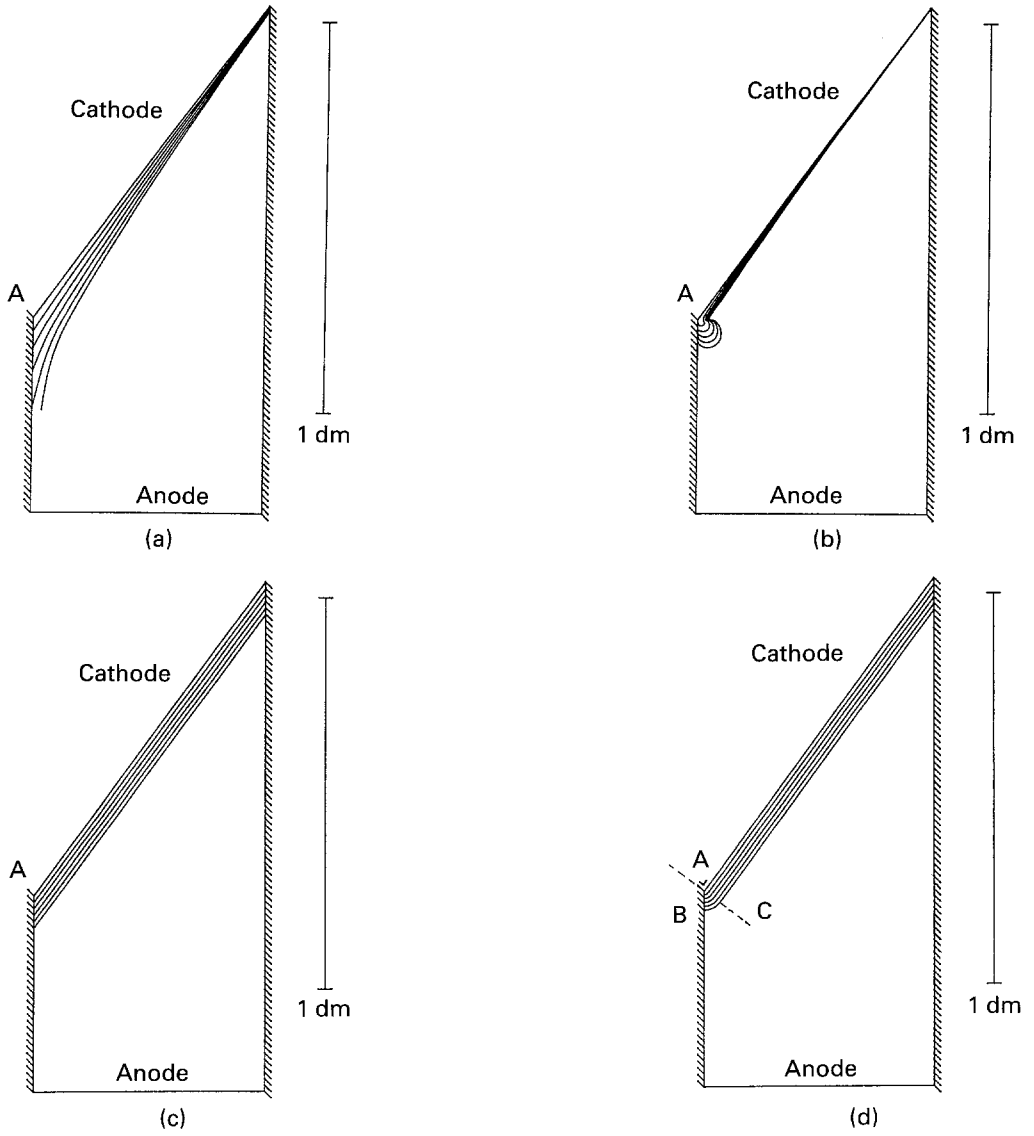

Fig. 3. Electrodeposition in a Hull cell simulated with extrapolation and connection of the electrode. Different Wagner numbers W are considered: (a) extrapolation $W = 0.5$, (b) connection $W = 0.005$, (c) extrapolation with uniform growth $W = 500$, and (d) connection with uniform growth $W = 500$.

at the fifth timestep, occurs immediately, since for a primary current density distribution, the current density at the lower electrode extremity is so high that no intersection with the insulating boundary could be found. In Fig. 3(c), due to the influence of a significant overvoltage, the current density distribution is uniform and so is the corresponding electrode growth. In Fig. 3(b) and (d) connection of the electrode extremities on successive timesteps, according to Fig. 2(b), was used. In Fig. 3(a) the current distribution is almost a primary distribution ($W = 0.005$). The small overpotential only influences the current density in a region very close to the singularity. In Fig. 3(d) the current density distribution and

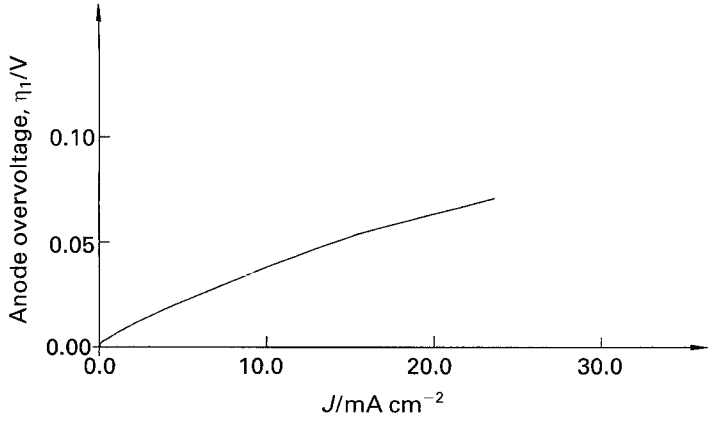

Fig. 4. Reduction of copper: measured overpotential on cathode applied to simulate electrode deposition.

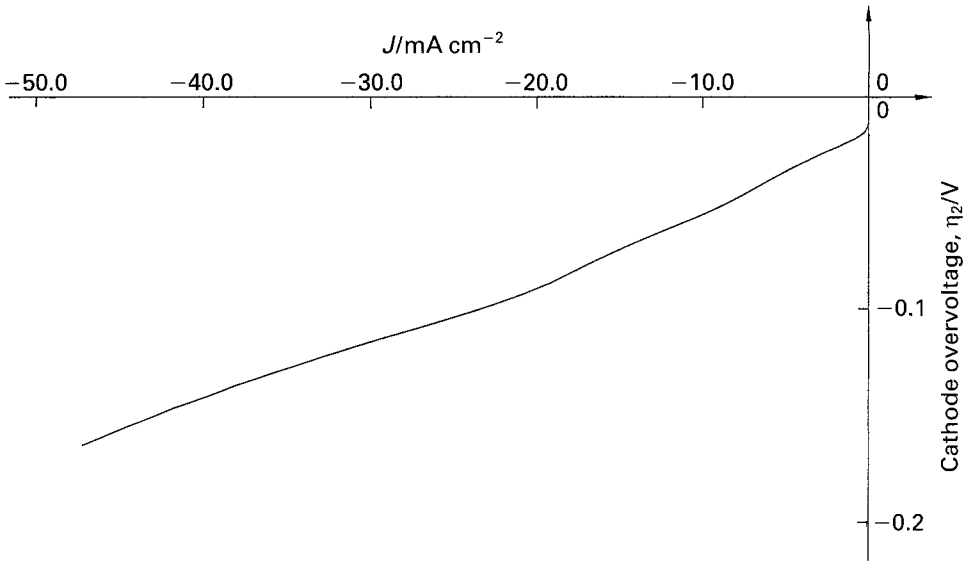

Fig. 5. Oxidation of copper: measured overpotential on anode applied to simulate electrode dissolution.

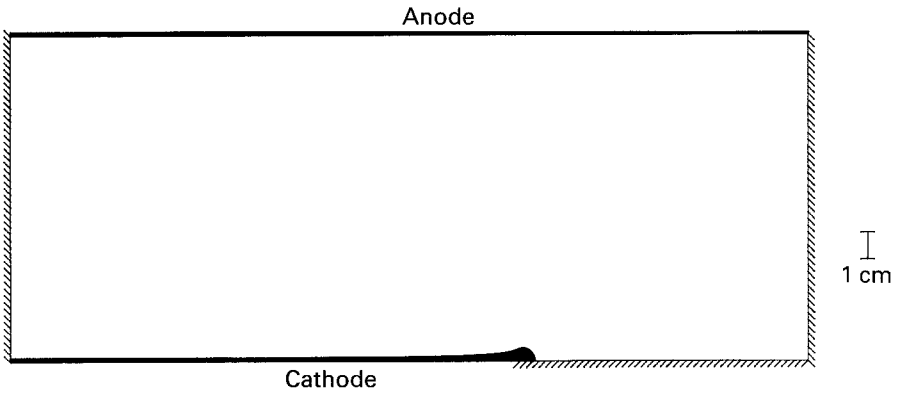

Fig. 6. Cell geometry with $\theta_0 = \pi$ and simulated profile history on anode (dissolution) and cathode (deposition).

the electrode growth are uniform due to the smoothing effect of the overvoltage ($W = 500$).

It is believed, regardless of the applied overvoltage, that the results obtained with connection of the electrode extremities at successive time steps, are much closer to reality. This can be rationalized as follows. In theory, when the Wagner number is strictly zero, near to the singularity point A, the only possible *electrical* stable situation is a growth towards a situation where 'at each moment' the angle between electrode and insulator is right. Indeed, when the angle is larger than $\pi/2$, it will increase after each time step since the current density at the extremity tends to infinity. On the other hand, once the angle becomes smaller than $\pi/2$ (there is no reason for this) the current density will be zero at the extremity and the angle of incidence will decrease to zero. A clear distinction has to be made between

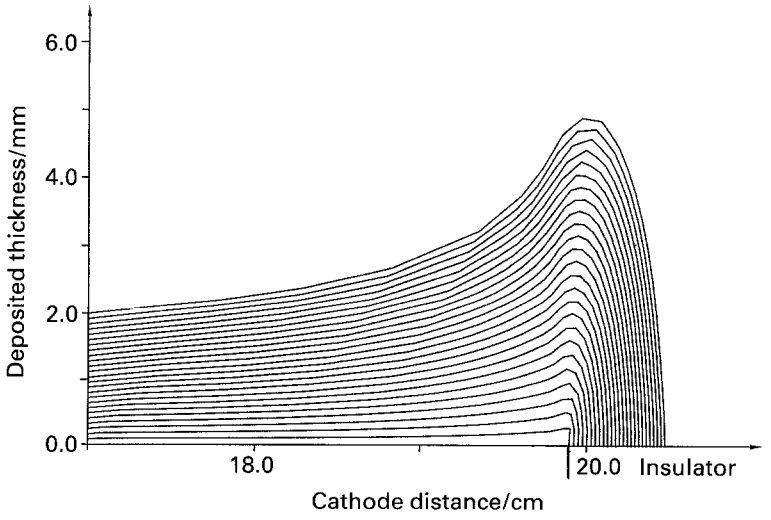

Fig. 7. Cell geometry of Fig. 6: simulated profile history near the singularity on the cathode ($\Delta t = 209$ min).

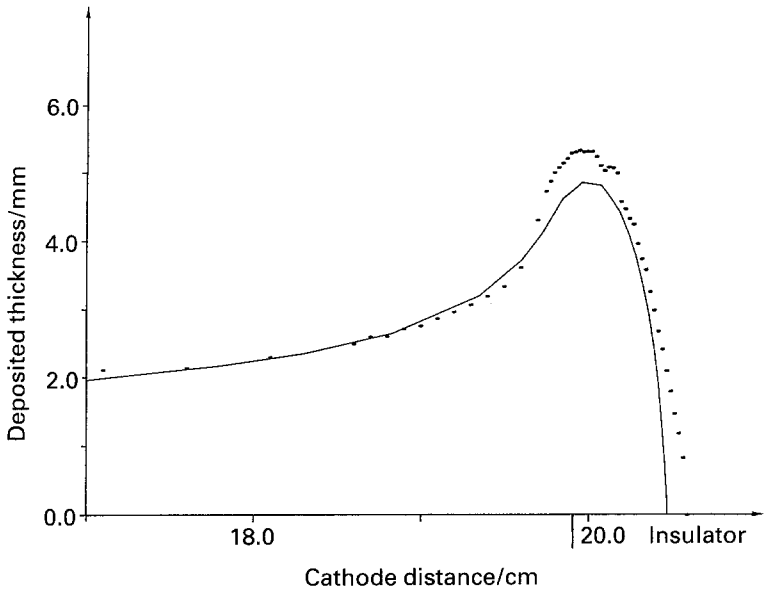

Fig. 8. Cell geometry of Fig. 6: comparison between measurement and simulation of deposited copper near the singularity.

the concept of electrical stability, valid at each moment, and the concept of stable deposit growth. As no dissolution of the anode is considered, depositing material on the cathode is, in fact, not stable, even in the case of a uniform compact deposit. Non-compact (e.g. dendritic) deposits are not considered here. The distance between both electrodes is always reduced by deposited metal such that, for a given potential difference, the current density and, consequently, the rate of metal deposition, will gradually increase, in theory up to short-circuit. It is obvious that for a primary current distribution once part of a cathode protrudes, it will grow faster and faster by attracting more and more current, as observed in Fig. 3(b).

When the current density is almost uniform (W is large), the electrode must grow uniformly in all directions. Hence, starting from the same point A (Fig. 3(d)), the points B and C, as well as all points on the electrode lying between B and C, must lie at the same distance from A. Between B and C the electrode profile should be part of a circle. This is approached using connection of the extremities. Simple extrapolation introduces a growth tangential to the electrode which makes no sense.

For $0 < W < \infty$, the same arguments exist and it may be concluded that for secondary distributions and starting from a singularity, the electrode profile will grown in such a way that the angle between the electrode and an adjacent insulator becomes and stays right. Therefore, but also because extrapolation is impossible when the electrode makes an angle with the boundary being $\geq \pi$, extrapolation is not acceptable and can give large errors. Due to the discretization of space and time, during simulations the incident angle can become somewhat smaller than $\pi/2$.

In the moving boundary algorithm presented by Ducovic, the gap is bridged with a circular arc having as centre point the electrode extremity on time step n and as radius the displacement of that electrode extremity. This method accepts inherently that the angle between an electrode and an adjacent insulator is right. Indeed, after the first timestep it is made right by construction. In contrast to the method of connection of the electrode extremities a certain overgrowth is also considered during the timestep. This corresponds with reality but for significant edge effects an overestimation is most probable when the timestep is (too) large. When sufficient small timesteps are applied, bridging a gap between two successive iterations by connection of the electrode extremities or by extrapolation with a circular arc will yield comparable results.

3. Comparison with experiment

To evaluate these numerical simulations and also because the growth out of a singularity in itself is a fascinating phenomenon, an experimental setup was built. The copper system was chosen to be a 0.8 M $CuSO_4$ (p.a)–0.8 M H_2SO_4 (p.a) solution containing 5 mg dm^{-3} thiourea in order to obtain smooth deposits. The electric resistivity of the electrolytic solution, measured with an impedance method, was 4.3 Ω cm at 25° C. The anodic and cathodic polarization curves (η_1 and η_2) were recorded on

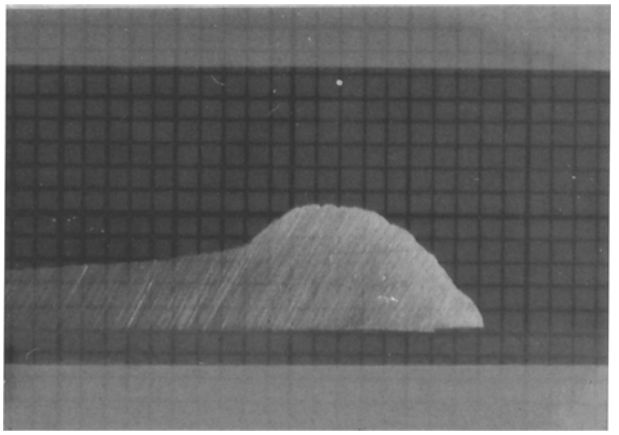

Fig. 9. Cell geometry of Fig. 6: picture of the deposited copper in the vicinity of the singularity ($\theta_0 = \pi$). The raster size is 1 mm^2.

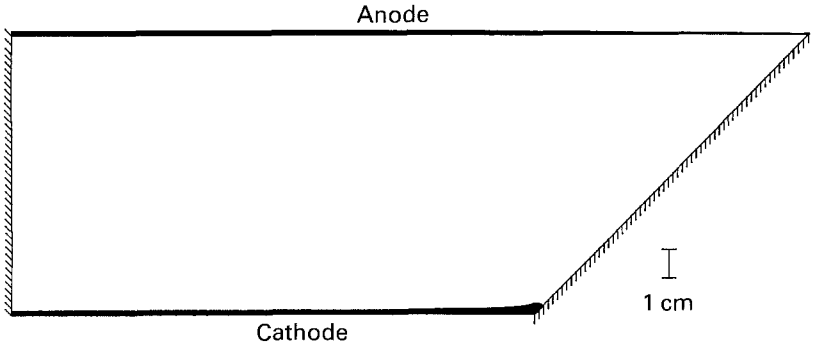

Fig. 10. Cell geometry with $\theta_0 = 3\pi/4$ and simulated profile history on anode and cathode. The anode dissolves whereas on the cathode copper is deposited.

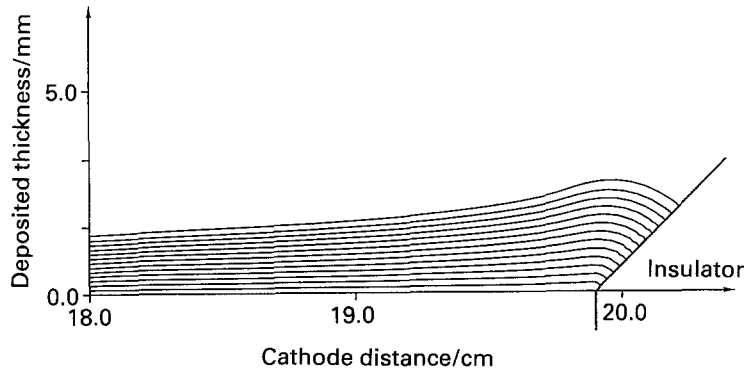

Fig. 11. Cell geometry of Fig. 10: simulated profile history near the singularity of the cathode ($\Delta t = 360$ min).

electrolytic pure copper (the same metal used for the growth experiments) with a conventional three-electrode configuration. Special care was taken to minimize ohmic voltage drop and it was investigated to what extent the overvoltages were independent on mass transport. The results are given in Figs 4 and 5. An approximation by cubic spline curves of these measured overvoltages was applied to model the nonlinear overvoltages during numerical growth simulations.

All measures were taken in order to have an ideal situation during the electrode growth experiments: constant temperature, removal of oxygen with nitrogen, maintaining a nitrogen blanket during experiments, rinsing of electrodes, no agitation, sufficiently low current density to ensure the conditions of a secondary current density distribution, warming-up of apparatus and preloading of the voltage source. Before and after each experiment, the electrodes were weighed. 100% efficiency was observed. After each experiment, the cathode was embedded in epoxy resin and cut to obtain several cross sections which were polished. Subsequently the profiles were measured using a Nikon-measure scope Model II having a precision of 0.001 mm. The final profile, used for comparison with calculations, was obtained by taking the mean value of at least three measured profiles. A given experiment was compared with a calculation for the same amount of charge. This means, that when the calculated total current was different from the measured one, the simulation time was adapted to have the same charge.

In Fig. 6 the cross section of the cell geometry with the simulated copper deposition on the cathode and copper dissolution on the anode are shown. Initially the angle between cathode and insulator (θ_0) was π. This experiment ran for 87.083 h, the applied voltage was 0.778 V. The total charge was 213.4 A h and the measured weight change of the cathode was 253.2 g.

In Fig. 7 the detail of the simulated profile history is given. It can be seen that at the first timestep two elements are introduced to connect both electrode extremities. Then the growth over the insulator is commenced. For the same experiment a comparison

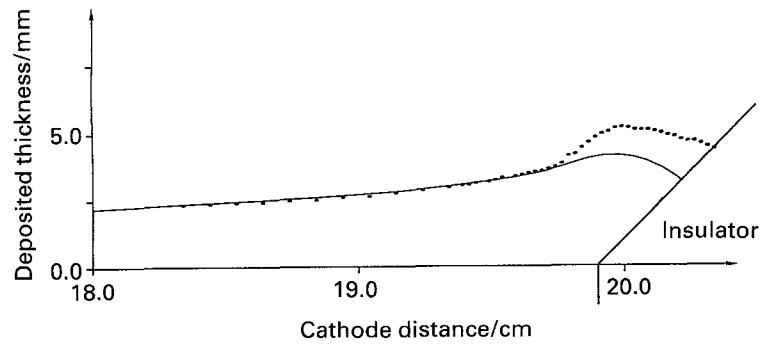

Fig. 12. Cell geometry of Fig. 10: comparison between measurement (●) and simulation (full line) of deposited copper near the singularity.

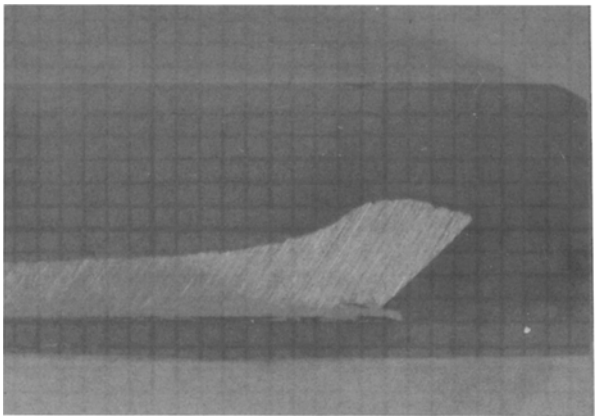

Fig. 13. Cell geometry of Fig. 10: picture of the deposited copper in the vicinity of the singularity $\theta_0 = 3\pi/4$. The raster size is 1 mm^2.

is made, in Fig. 8, between the experimental and simulated profile. The final electrode profile obtained in the experiment is shown in Fig. 9. Clearly, the theoretical and numerical results are in good agreement. Several other experiments were performed with varying applied voltages and electrode distances. In all cases the predicted electrode evolution was in good agreement with the experiments.

Figure 10 shows the case where the initial angle (θ_0) between the extremity of the cathode and the adjacent insulator is $3\pi/4$. The experiment ran for 79.15 h, the applied voltage was 0.803 V. The total charge was 215.57 A h and the measured weight change of the cathode was 256.4 g.

In Figs 11 and 12 a detail of the simulated profile history and the comparison with the corresponding experiment are given. Figure 13 represents the final profile.

In the more uniform parts, away from the singularities, the difference between simulations and experiments can be attributed to errors involved by measurement (conductivity, polarization curves, current, voltage, profiles) and surface roughness. Near to a singularity, the surface roughness was more pronounced. This causes larger measuring errors but also indicates that phenomena such as mass transport, not considered in these simulations, might become important.

5. Conclusion

Even in the vicinity of singularities, mathematical modelling of electrodeposition is possible provided that the electrode extremities between two successive timesteps are interconnected. These simulations provide acceptable agreement with experimental results. Phenomena such as overgrowth, overshoot, and the fact that the angle of incidence between an electrode and an insulator becomes perpendicular, are well described.

References

[1] J. Newman, 'Electrochemical Systems', Prentice Hall, Englewood Cliffs, NJ (1973).

[2] J. A. McGeough, 'Principles of Electrochemical Machining'. Chapman & Hall, London (1974).

[3] J. Deconinck, G. Maggetto, P. Versyck and J. Vereecken, 'The Boundary Element Method (BEM) for Calculation of Current Distributions in Electrochemical Systems'. Extended abstracts of the 34th ISE Meeting, Erlangen, BRD (1983).

[4] G. Finoly, A. Gernay and A. Giroud, 'Application and Validation of the Boundary Element Method to Cathodic Protection Designs on Vessels', XIVth International Conference on Boundary Element Methods, Vol. 1, Sevilla, Nov. (1992) pp. 423–435.

[5] F. Brichau and J. Deconinck, 'A numerical model for cathodic protection of buried pipe lines', accepted for publication in *Corrosion* (NACE).

[6] J. Deconinck, 'Current Distribution and Electrode Shape Changes in Electrochemical Systems – a Boundary Element Approach', Lecture Notes in Engineering no. 75, Springer-Verlag (1992).

[7] N. G. Zamani and J. M. Chuang, Electroplating, *in* 'Topics in Boundary Element Research', Vol. 7, Electrical Engineering Applications, Springer-Verlag (1990) Chapter 6.

[8] G. A. Prentice, 'Modeling of Changing Electrode Profiles', Ph.D thesis, Lawrence Berkeley Laboratory, University of California (1980).

[9] J. Ducovic and C. W. Tobias, *J. Electrochem. Soc.*, **137** (1990) 3748–3755.